Journal of Solid State Chemistry 183 (2010) 1334–1339

Contents lists available at ScienceDirect

Journal of Solid State Chemistry

journal homepage: www.elsevier.com/locate/jssc

Synthesis, crystal structure, and structural conversion of Ni molybdate hydrate $NiMoO_4 \cdot nH_2O$

Kazuo Eda [a,*], Yasuyuki Kato [a], Yu Ohshiro [a], Takamitu Sugitani [a], M. Stanley Whittingham [b]

[a] Department of Chemistry, Graduate School of Science, Kobe University, Nada-ku, Kobe 657-8501, Japan
[b] Institute for Materials Research, State University of New York at Binghamton, Binghamton, NY 13902-6000, USA

ARTICLE INFO

Article history:
Received 7 December 2009
Received in revised form
2 April 2010
Accepted 9 April 2010
Available online 13 April 2010

Keywords:
Ni molybdate hydrate
Crystal structure
Structural conversion
Hydrothermal synthesis

ABSTRACT

The synthesis and crystal structure of $NiMoO_4 \cdot nH_2O$ were investigated. The hydrate crystallized in the triclinic system with space group $P-1$, $Z=4$ with unit cell parameters of $a=6.7791(2)$ Å, $b=6.8900(2)$ Å, $c=9.2486(2)$ Å, $\alpha=76.681(2)^\circ$, $\beta=83.960(2)^\circ$, $\gamma=74.218(2)^\circ$. Its ideal chemical composition was $NiMoO_4 \cdot 3/4H_2O$ rather than $NiMoO_4 \cdot 1H_2O$. Under hydrothermal conditions the hydrate turned directly into α–$NiMoO_4$ above 483 K, giving nanorods thinner than the crystallites of the mother hydrate. On the other hand, it turned into Anderson type of polyoxomolybdate via a solid-solution process in a molybdate solution at room temperature.

1. Introduction

Ni molybdates are attractive compounds because of their structural, magnetic, catalytic, and electrochemical (Li storage) properties [1–13]. These properties depend not only on their compositions and structures but also on their particle's morphology and size. It has been known that preparation methods and conditions become key elements to control these materials parameters [14–16].

Ni molybdate hydrates $NiMoO_4 \cdot nH_2O$ are often utilized as a precursor for preparing the corresponding molybdates. In order to produce well-designed Ni molybdates, it is essential to know the details of the structure and structural conversion of the hydrate. However, the hydrate tends to precipitate in poorly crystalline forms [9,17], and the determination of its crystal structure is difficult, like some other transition metal molybdate hydrates $MMoO_4 \cdot nH_2O$ (M=Co, Fe). Thus, the crystal structure of $NiMoO_4 \cdot nH_2O$ is still unknown, although that of $CoMoO_4 \cdot nH_2O$ ($n=3/4$) was determined by us recently [18].

In an ongoing study we have investigated the synthesis, crystal structure, and structural conversion of $NiMoO_4 \cdot nH_2O$ and succeeded in obtaining $NiMoO_4 \cdot nH_2O$ with high crystallinity via a hydrothermal route. Very recently Ding et al. reported another hydrothermal synthesis and concluded that its composition was $NiMoO_4 \cdot H_2O$ ($n=1$) [19]. However, the XRD patterns of their $NiMoO_4 \cdot nH_2O$ samples, identified as a single-phase and as a mixture with $Ni_2(NO_3)_2(OH)_2 \cdot nH_2O$, are very similar to those of our $CoMoO_4 \cdot 3/4H_2O$ samples with low and high crystallinity, respectively (Fig. S1 of Supporting Information), indicating that $NiMoO_4 \cdot nH_2O$ is isostructural with $CoMoO_4 \cdot 3/4H_2O$. The present paper focuses on the synthesis and crystal structure of $NiMoO_4 \cdot nH_2O$, comparing with the products of Ding et al.'s method. Structural conversions of $NiMoO_4 \cdot nH_2O$ are also described.

2. Experimental

$NiMoO_4 \cdot nH_2O$ was synthesized by a hydrothermal technique. Special grades of $Ni(NO_3)_2 \cdot 6H_2O$ and $(NH_4)_6Mo_7O_{24} \cdot 4H_2O$ were purchased from Wako Pure Chemical Industries, Ltd. and used as the Ni and Mo sources without further purification. The Ni and Mo sources (for details, see Section 3.1) were dissolved or suspended in 15 mL of water. The resulting solution was put into a 25 mL Teflon-lined autoclave and heated in a forced convection oven at desired temperatures under autogenous pressure for desired times. The resulting product was filtered, washed with distilled water, and dried in air at room temperature.

Powder X-ray diffraction of the product was measured on a Mac Science MXP3VZ X-ray diffractometer with a graphite monochromator using Cu$K\alpha$ radiation. Step-scan recordings at 0.02° step sizes and 6s counting times were used for the Rietveld analysis. The Rietveld analysis of the diffraction pattern was performed using Rietan 2000 [20]. The chemical compositions of the products were determined by inductively coupled plasma atomic emission spectroscopy (ICP, SHIMAZU 7510) and thermogravity-differential thermal analysis (TG-DTA, MAC SCIENCE

* Corresponding author. Fax: +81 78 803 5677.
E-mail address: eda@kobe-u.ac.jp (K. Eda).

0022-4596/$ - see front matter © 2010 Elsevier Inc. All rights reserved.
doi:10.1016/j.jssc.2010.04.009

2010S system). TG-DTA measurements were performed in nitrogen at a heating rate of 10 K min^{-1}. FT-IR spectra of the samples were measured on a Perkin-Elmer Spectrum 1000 FT-IR spectrometer using the KBr pellet method. SEM observations of the products were performed on a JEOL JSM-5610LVS scanning electron microscope.

3. Results and discussion

3.1. Hydrothermal syntheses

In our previous study [18], we successfully prepared single crystals of $CoMoO_4 \cdot 3/4H_2O$ by a hydrothermal treatment of CoO suspended in an aqueous $MoO_3 \cdot nH_2O$ solution. In the present work a similar hydrothermal synthesis that utilized NiO instead of CoO was performed to obtain $NiMoO_4 \cdot nH_2O$ at first. The resulting products exhibited XRD peaks similar to those of $CoMoO_4 \cdot 3/4H_2O$, but always contained some unchanged NiO. Although the molar ratio of $NiO/MoO_3 \cdot nH_2O$ in the suspension solution, treatment temperature (up to 473 K), and treatment time (up to 1 week) were variously changed, the products without unchanged NiO could not be obtained as long as NiO and $MoO_3 \cdot nH_2O$ were used as starting materials. The residual NiO problem was solved by using amorphous $NiMoO_4 \cdot nH_2O$ as a starting material instead of the mixture of NiO and $MoO_3 \cdot nH_2O$. Amorphous $NiMoO_4 \cdot nH_2O$ (green-yellow in color) was prepared by mixing equivalent molar amounts of $Ni(NO_3)_2 \cdot 6H_2O$ and $(NH_4)_6Mo_7O_{24} \cdot 4H_2O$, grinding in a mortar with a pestle, calcining in 453 K for 1 day, washing with water, and drying in air. The single phase of crystalline $NiMoO_4 \cdot nH_2O$ (whitish yellow), structural details of which are described below, could be obtained typically by a hydrothermal treatment of 1 g of amorphous $NiMoO_4 \cdot nH_2O$ suspended in 15 mL water at 453 K for 1 day. The quantitative yield was ca. 45% (by weight, based on Mo). The XRD pattern of the resulting $NiMoO_4 \cdot nH_2O$ (hereafter denoted as 'Eda-hydrothermal') is shown in Fig. 1a.

To compare with 'Eda-hydrothermal', two other $NiMoO_4 \cdot nH_2O$ samples (whitish yellow) were also prepared from $Ni(NO_3)_2$+$(NH_4)_6Mo_7O_{24}$ solutions, whose pH values were adjusted to 7 and 5, respectively, according to the Ding et al.'s method. Because their yields were rather low compared to that of 'Eda-hydrothermal', we investigated the syntheses from solutions with higher $Ni(NO_3)_2$+$(NH_4)_6Mo_7O_{24}$ concentration than the original values of the Ding et al.'s method. Products consistent with Ding et al.'s results could be obtained from the pH 5 solution with up to nine times as high a concentration as that of the original $Ni(NO_3)_2$+$(NH_4)_6Mo_7O_{24}$ concentration, and up to twice for the pH 7 solution. In this investigation an interesting structural conversion of $NiMoO_4 \cdot nH_2O$ via a solid-solution reaction was found in the pH 5 solution with the higher $Ni(NO_3)_2$+$(NH_4)_6Mo_7O_{24}$ concentration, and will be described later.

The XRD patterns of these two $NiMoO_4 \cdot nH_2O$ samples (denoted as 'Ding-pH7' and 'Ding-pH5', respectively) are also shown in Fig. 1. The three XRD patterns shown are identical with one another, except that the pattern of 'Ding-pH7' is broad and structure-less. According to SEM observations (Fig. 2), the particle size of the sample 'Ding-pH7' is much smaller than those of the other two $NiMoO_4 \cdot nH_2O$ samples. These three samples also exhibit similar IR

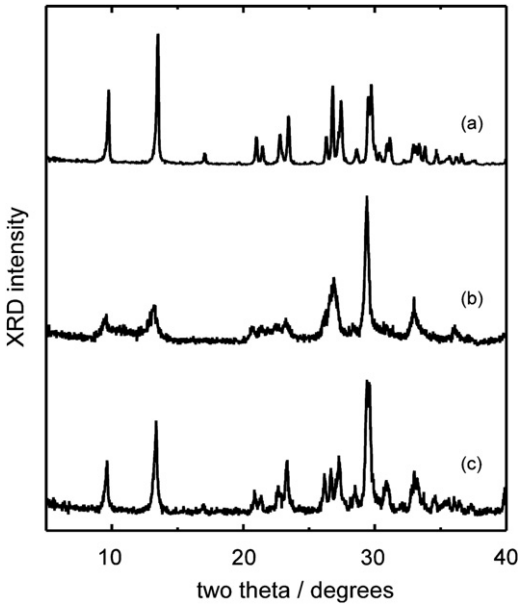

Fig. 1. XRD patterns of $NiMoO_4 \cdot nH_2O$ samples: 'Eda-hydrothermal' (a), 'Ding-pH7' (b), 'Ding-pH5' (c).

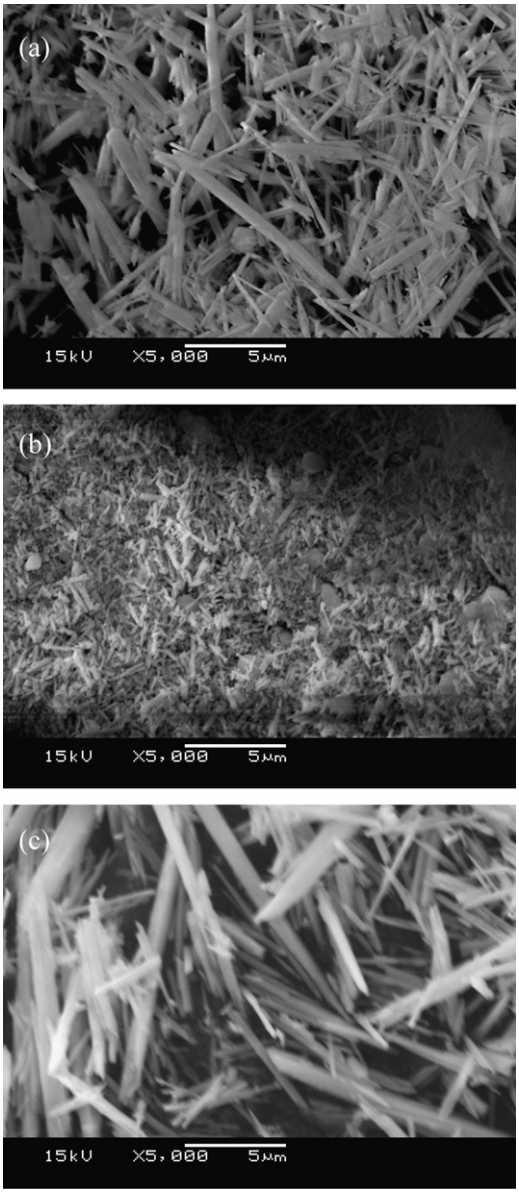

Fig. 2. SEM images of $NiMoO_4 \cdot nH_2O$ samples: 'Eda-hydrothermal' (a), 'Ding-pH7' (b), 'Ding-pH5' (c).

spectra to each other (Fig. 3), but that of 'Ding-pH7' apparently includes some spectral differences from those of the other two in the range of 800–850 cm^{-1}, indicating the differences in local structures. Table 1 shows the results of compositional analyses for these three samples, together with their yields. According to the results, all three are best described as $NiMoO_4 \cdot 3/4H_2O$ rather than $NiMoO_4 \cdot 1H_2O$, but it should be noted that 'Ding-pH7' includes extra portion of NiO unlike the other two samples.

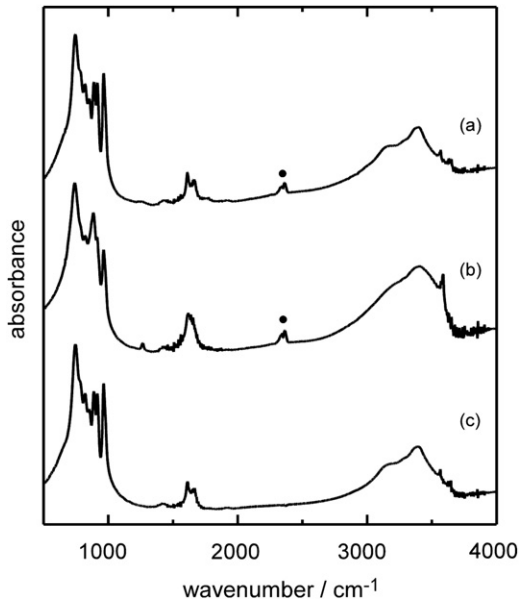

Fig. 3. IR spectra of $NiMoO_4 \cdot nH_2O$ samples: 'Eda-hydrothermal' (a), 'Ding-pH7' (b), 'Ding-pH5' (c). Double peaks marked with symbol ● are due to CO_2 in air.

3.2. Crystal structure of the $NiMoO_4 \cdot nH_2O$

In spite of our efforts no crystals suitable for single crystal X-ray analysis were obtained. However, the crystal structure of $NiMoO_4 \cdot nH_2O$ could be determined by powder Rietveld analysis, because the XRD pattern of 'Eda-hydrothermal' agreed well with the pattern simulated using the atomic parameters of $CoMoO_4 \cdot 3/4H_2O$ [18] (with Co replaced by Ni). Fig. 4 shows the results of Rietveld analysis of the XRD pattern. Table 2 lists the atomic parameters. The (triclinic) lattice constants refined were $a=6.7791(2)$ Å, $b=6.8900(2)$ Å, $c=9.2486(2)$ Å, $\alpha=76.681(2)^\circ$, $\beta=83.960(2)^\circ$, $\gamma=74.218(2)^\circ$ (space group $P-1$, $Z=4$). All atoms were refined isotropically and all the oxygen atoms except for O2*w* were refined with a common atomic displacement parameter. Occupanciy of O2*w* was fixed so as to match the real composition $NiMoO_4 \cdot 0.70H_2O$ of 'Eda-hydrothermal', in which ca. 20% lattice water (O2*w*) was absent. The agreement factors were *R*wp=9.40% and *R*p=7.28%, respectively with the Goodness-of-fit $S=2.76$, indicating a fairly good fit.

The resulting structure consists of tetrameric *z*-shaped unit of Ni octahedra, two NiO_6 and two $NiO_5(OH_2)$, that share edges (Fig. 5). These units are interconnected by MoO_4 tetrahedra to form a network structure having open channels. The coordination water (O1*w*) of $NiO_5(OH_2)$ projects into the channel, and

Table 1
Chemical compositions (Ni and Mo contents) and yields of $NiMoO_4 \cdot nH_2O$ samples.

$NiMoO_4 \cdot nH_2O$ samples	'Eda-hydrothermal'	'Ding-pH7'[a]	'Ding-pH5'[b]
Mo content, wt% found (Calcd)	41.6 (41.3[c], 40.5[d])	39.6 (41.3[c], 40.5[d])	41.9 (41.3[c], 40.5[d])
Ni content, wt% found (Calcd)	25.7 (25.3[c], 24.8[d])	27.1 (25.3[c], 24.8[d])	25.9 (25.3[c], 24.8[d])
[Ni]/[Mo] molar ratio	1.01	1.12	1.01
n[e]	0.70	0.84	0.78
Composition	$NiMoO_4 \cdot nH_2O$	$Ni_{1.12}MoO_{4.12} \cdot nH_2O$	$NiMoO_4 \cdot nH_2O$
Yield[f] (%)	45.2	19.6	11.4

[a] Prepared from the solution with five times the original $Ni(NO_3)_2$+$(NH_4)_6Mo_7O_{24}$ concentration of the Ding et al.'s method [19].
[b] From the solution with twice the original concentration.
[c] Calculated for $NiMoO_4 \cdot 3/4H_2O$.
[d] For $NiMoO_4 \cdot 1H_2O$.
[e] Evaluated from the TG-DTA results.
[f] Based on Mo.

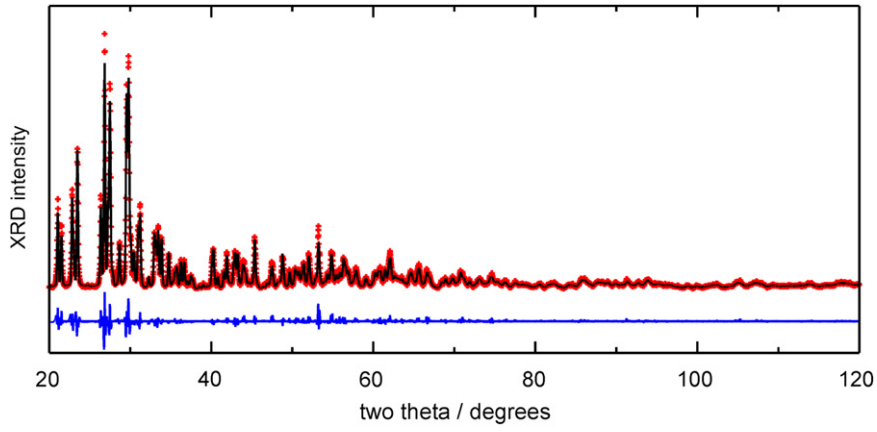

Fig. 4. The Rietveld refinement plot of the $NiMoO_4 \cdot nH_2O$ sample 'Eda-hydrothermal'. Continuous line corresponds to the calculated pattern, the small crosses (+) the observed values. The bottom trace depicts the differential plot of experimental and calculated intensities.

Table 2
Atomic parameters for $NiMoO_4 \cdot nH_2O$.

Atom	Site	x	y	z	Occupancy	B (Å^2)
Ni1	2*i*	0.8088(6)	1.1704(6)	0.0279(4)	1	0.50
Ni2	2*i*	0.8449(6)	0.3525(6)	0.3003(4)	1	0.42
Mo1	2*i*	0.9957(4)	0.8056(4)	0.3164(2)	1	0.72
Mo2	2*i*	0.7527(3)	0.7060(3)	−0.0526(3)	1	0.25
O1	2*i*	1.0911(18)	0.774(2)	0.4924(14)	1	0.53
O2	2*i*	1.2232(19)	0.7357(19)	0.1996(13)	1	0.53
O3	2*i*	0.49058(18)	0.809(2)	−0.0668(13)	1	0.53
O4	2*i*	0.854(2)	0.6893(19)	−0.2352(14)	1	0.53
O5	2*i*	0.858(2)	1.077(2)	0.2547(15)	1	0.53
O6	2*i*	0.8373(18)	0.636(2)	0.3308(14)	1	0.53
O7	2*i*	0.8687(19)	0.870(2)	0.0140(14)	1	0.53
O8	2*i*	0.804(2)	0.450(2)	0.0685(13)	1	0.53
O1*w*	2*i*	0.5358(18)	0.408(2)	0.3580(14)	1	0.53
O2*w*	2*i*	0.492(8)	−0.005(8)	0.466(4)	0.40	0.74

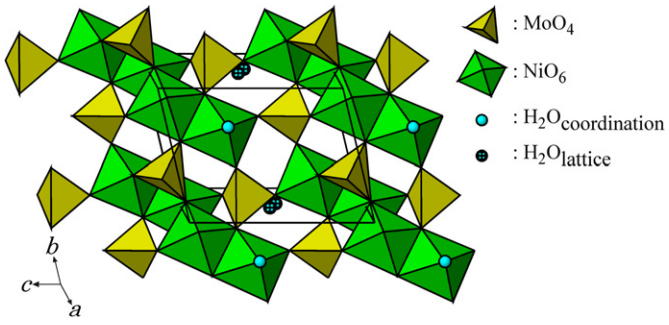

Fig. 5. Crystal structure of the $NiMoO_4 \cdot nH_2O$.

Table 3
Averaged lengths of *M*–O bonds in respective polyhedra.

Hydrates	Polyhedra	Averaged lengths (Å)
$NiMoO_4 \cdot 3/4H_2O$		
	NiO_6	2.06
	$NiO_5(OH_2)$	2.03
	MoO_4–(1)	1.79
	MoO_4–(2)	1.78
$CoMoO_4 \cdot 3/4H_2O$		
	CoO_6	2.08
	$CoO_5(OH_2)$	2.09
	MoO_4–(1)	1.75
	MoO_4–(2)	1.74
$FeAsO_4 \cdot 3/4H_2O$		
	FeO_6	2.02
	$FeO_5(OH_2)$	2.01
	AsO_4–(1)	1.69
	AsO_4–(2)	1.68

additional lattice water (O2*w*) is included in it. This structure is isostructural with those of $Fe(III)AsO_4 \cdot 3/4H_2O$[21] as well as $CoMoO_4 \cdot 3/4H_2O$[18]. The averaged lengths of *M*–O bonds (*M*=Ni, Co, Fe, Mo, As) for respective polyhedra MO_n or $MO_{n-1}(OH_2)$ are summarized in Table 3. According to Kolitsch and Schwendtner [22,23], there is a similar isotypic relationship between *M*(III)-arsenate hydrates and *M*(II)-molybdate hydrate.

3.3. Structural conversion of $NiMoO_4 \cdot nH_2O$

3.3.1. In ambient atmosphere

This hydrate exhibits two kinds of dehydrations (at 350–540 and 540–700 K, Fig. 6). The first one (due to 'lattice water') is reversible, and the structure of the hydrate remains after this dehydration (Fig. 7). It was also confirmed that the structure remained even when the hydrate was heated at 533 K for 24 h. The second one (due to 'coordination water') is irreversible, and is accompanied by an exotherm at 693 K, which is due to a structural conversion of the hydrate (Fig. 7). Morphologies of particles of the hydrate remain after this conversion (Fig. 8a and b). We suggest that this exotherm is related to the structural conversion to β-$NiMoO_4$, as described in previous papers [13], although the post TG-DTA sample heated up to 773 K shows the XRD pattern of α-$NiMoO_4$ (Fig. 7). A small exothermal DTA peak observed at ca. 500 K on a cooling run after being heated up to 773 K (Fig. S2 of Supporting Information) confirmed that the hydrate turned into β-$NiMoO_4$ on heating and then to α-$NiMoO_4$ on cooling to room temperature. This suggestion agrees with the previous report that β-$NiMoO_4$ tuned into α-$NiMoO_4$ at around 473 K on cooling [13].

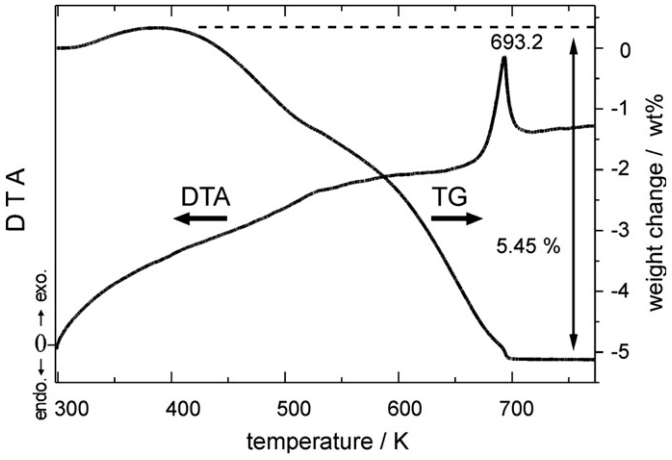

Fig. 6. TG-DTA curves of the $NiMoO_4 \cdot nH_2O$ sample 'Eda-hydrothermal'.

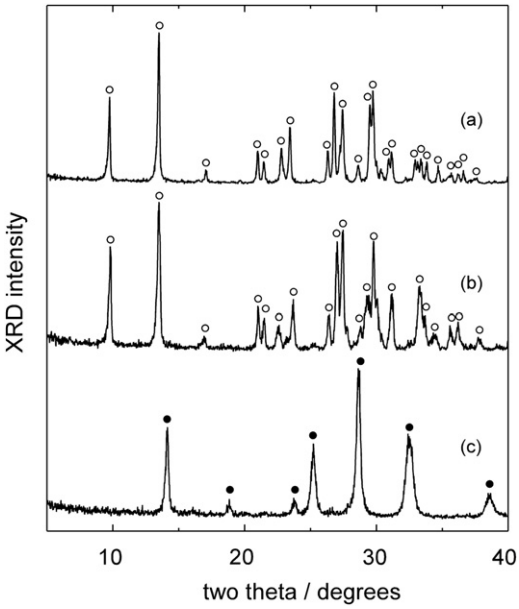

Fig. 7. XRD patterns of the $NiMoO_4 \cdot nH_2O$ sample 'Eda-hydrothermal' (a) and its post-TGDTA products heated at 623 K (b) and 773 K (c). Symbols ○ and ● indicate $NiMoO_4 \cdot 3/4H_2O$ and α–$NiMoO_4$, respectively.

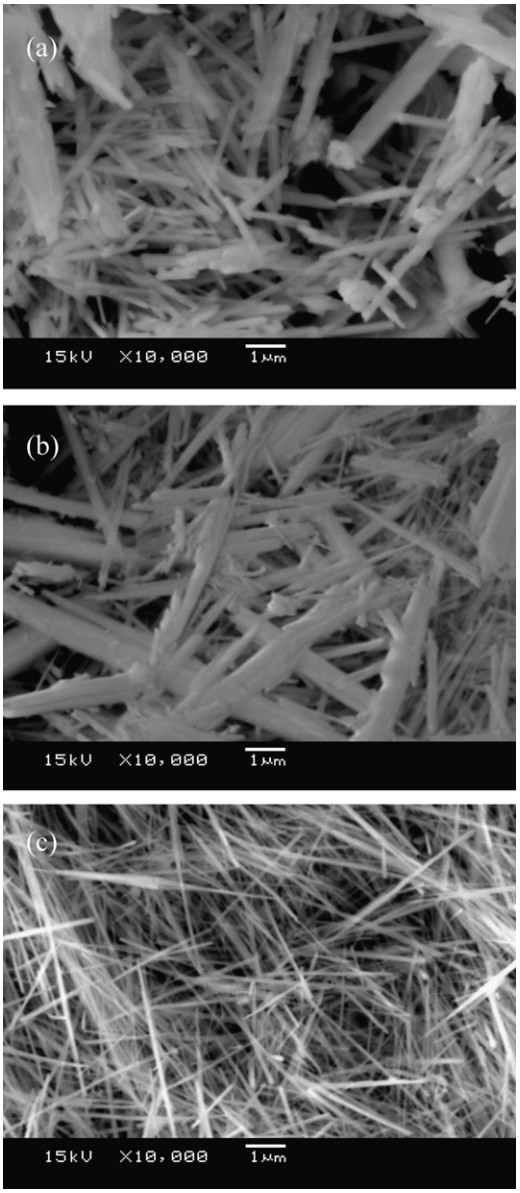

Fig. 8. SEM images of $NiMoO_4 \cdot nH_2O$ sample 'Eda-hydrothermal' (a), its post-TGDTA product heated at 773 K (b), and the hydrothermal product treated at 533 K for 1 day (c).

3.3.2. Under hydrothermal condition

Recently we found that $CoMoO_4 \cdot 3/4H_2O$ turned into a high-pressure phase of $CoMoO_4$ (hp–$CoMoO_4$) at a lower pressure and temperature (453 K and ca. 10 bar) [24] than those (ca. 900 K and 50 kbar) necessary for the usual formation of hp–$CoMoO_4$ [25]. Expecting a similar conversion of $NiMoO_4 \cdot nH_2O$ to hp–$NiMoO_4$, we investigated the dehydration of $NiMoO_4 \cdot nH_2O$ under hydrothermal conditions. In the present study any evidence of the conversion could not be found, but α-$NiMoO_4$ (whitish yellow) was formed from $NiMoO_4 \cdot nH_2O$ at above 483 K (Fig. 9). Because this formation temperature of α-$NiMoO_4$ is lower than the temperature of the transformation from β-$NiMoO_4$ to α-$NiMoO_4$, the formation of α-$NiMoO_4$ under the hydrothermal conditions may be achieved directly from $NiMoO_4 \cdot nH_2O$ without passing into β-$NiMoO_4$, unlike in an ambient atmosphere. Furthermore, it should be noted that the resulting α-$NiMoO_4$ is formed as nanorods much thinner than the crystallites of the mother hydrate, according to the SEM investigations (Fig. 8a and c).

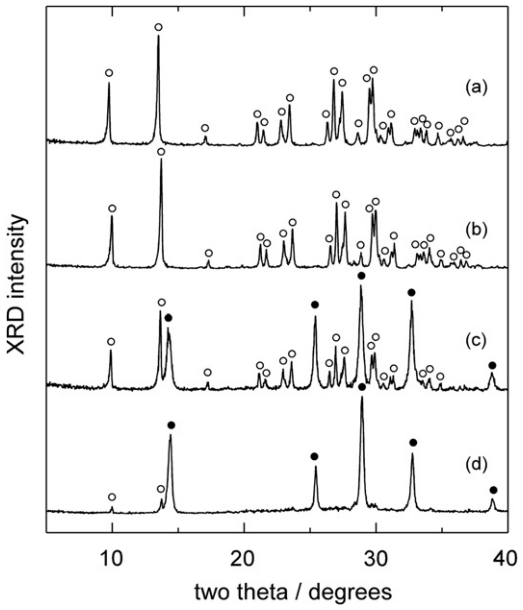

Fig. 9. XRD patterns of $NiMoO_4 \cdot nH_2O$ sample 'Eda-hydrothermal' (a), and its hydrothermal products treated at 453 K for 1 week (b), at 483 K for 3 days (c), and at 533 K for 1 day (d). Symbols ○ and ● indicate $NiMoO_4 \cdot 3/4H_2O$ and α–$NiMoO_4$, respectively.

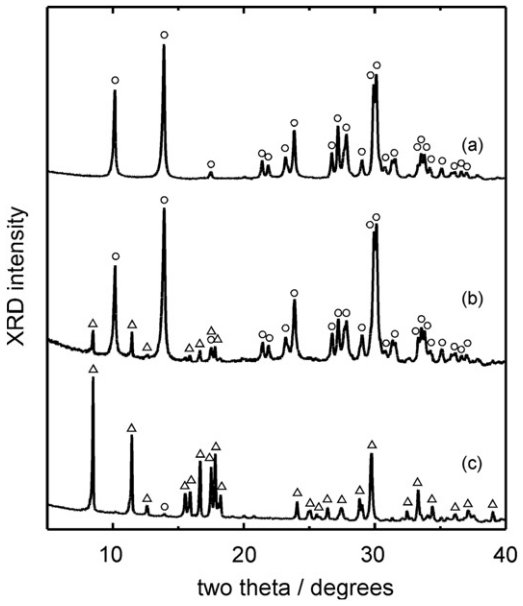

Fig. 10. XRD patterns of the products obtained when cooled down to 323 K (a), to room temperature (b), and subsequently aged at room temperature for 1 day (c) after the Ding et al.'s hydrothermal synthesis (pH 5, five times the original $Ni(NO_3)_2$+$(NH_4)_6Mo_7O_{24}$ concentration). Symbols ○ and Δ indicate $NiMoO_4 \cdot 3/4H_2O$ and $(NH_4)_4H_6NiMo_6O_{24} \cdot 4H_2O$, respectively.

3.3.3. In aqueous solution

As mentioned above, we found an interesting reaction of $NiMoO_4 \cdot nH_2O$ occurred via a solid-solution process. According to the XRD patterns of the products (Fig. 10), $NiMoO_4 \cdot nH_2O$ turns into $(NH_4)_4H_6NiMo_6O_{24} \cdot 4H_2O$ (whitish blue), which consists of Anderson type of polyoxomolybdate anions, when the hydrate is kept in the resulting supernatant solution at room temperature for a long time. It was confirmed that no precipitate was obtained only from the solution at room temperature. This fact indicates that the

conversion of $NiMoO_4 \cdot nH_2O$ to $(NH_4)_4H_6NiMo_6O_{24} \cdot 4H_2O$ proceeds via a solid-solution process. Furthermore, it was confirmed that the hydrate turned into $(NH_4)_4H_6NiMo_6O_{24} \cdot 4H_2O$ in 1M $(NH_4)_6Mo_7O_{24}$ aqueous solution at room temperature, but that its structure remained same in water.

4. Conclusion

The synthesis and crystal structure of $NiMoO_4 \cdot nH_2O$ were investigated. $NiMoO_4 \cdot nH_2O$ with high crystallinity could be obtained from amorphous $NiMoO_4 \cdot nH_2O$, which was prepared by calcining a mixture of $Ni(NO_3)_2 \cdot 6H_2O$ and $(NH_4)_6Mo_7O_{24} \cdot 4H_2O$, via a hydrothermal route. From the compositional and structural analyses, it could be concluded that the hydrate had a chemical composition of $NiMoO_4 \cdot 3/4H_2O$ rather than $NiMoO_4 \cdot 1H_2O$. The hydrate consisted of tetrameric *z*-shaped unit of Ni octahedra and MoO_4 tetrahedra, and had a network structure having open channels. The crystal structure was isostructural with $Fe(III)AsO_4 \cdot 3/4H_2O$ as well as $CoMoO_4 \cdot 3/4H_2O$. Some kinds of conversions of $NiMoO_4 \cdot nH_2O$ were newly revealed. $NiMoO_4 \cdot nH_2O$ turned directly into α-$NiMoO_4$ at above 483 K under hydrothermal conditions. The resulting α-$NiMoO_4$ was formed as nanorods thinner than crystallites of the mother hydrate. Furthermore, $NiMoO_4 \cdot nH_2O$ turned into $(NH_4)_4H_6NiMo_6O_{24} \cdot 4H_2O$, which consists of Anderson type of polyoxomolybdate anions, via a solid-solution process in an molybdate solution at room temperature.

Acknowledgment

The work at Kobe was supported by Grant-in-Aid for Scientific Research(C) 20550176, and the work at Binghamton was supported by the National Science Foundation under grant DMR-0705657.

Appendix A. Supplementary material

Supplementary data associated with this article can be found in the online version at doi:10.1016/j.jssc.2010.04.009.

References

[1] A.P. Young, C.M. Schwartz, Science 141 (1963) 348.
[2] A.W. Sleight, B.L. Chamberland, Inorg. Chem. 7 (1968) 1672.
[3] K.T. Jacob, G.M. Kale, G.N.K. Iyengar, J. Mater. Sci. 22 (1987) 4274.
[4] M. Wiesmann, H. Ehrenberg, G. Wltschek, P. Zinn, H. Weitzel, H. Fuess, J. Magn. Magn. Mater. 150 (1995) L1.
[5] K.T. Jacob, S.V. Varamban, J. Alloys Compd. 280 (1998) 138.
[6] C. Livage, A. Hynaux, J. Marot, M. Nogues, G. Férey, J. Mater. Chem. 12 (2002) 1423.
[7] C. Mazzocchia, C. Aboumrad, C. Diagne, E. Tempesti, J.M. Herrmann, G. Thomas, Catal. Lett. 10 (1991) 181.
[8] J. Zou, G.L. Schrader, J. Catal. 161 (1996) 667.
[9] J.L. Brito, A.L. Barbosa, J. Catal. 171 (1997) 467.
[10] J.A. Rodriguez, S. Chaturvedi, J. Hanson, A. Albornoz, J.L. Brito, J. Phys. Chem. B 102 (1998) 1347.
[11] J.A. Rodriguez, S. Chaturvedi, J. Hanson, A. Albornoz, J.L. Brito, J. Phys. Chem. B 103 (1999) 770.
[12] R.N. Singh, Madhu, R. Awasthi, A.S.K. Sinha, J Solid State Electrochem. 13 (2009) 1613.
[13] W. Xiao, J.S. Chen, C.M. Li, R. Xu, X.W. Lou, Chem. Mater. (in press) (doi:10.1021/cm9012014).
[14] J.G. Li, T. Ishigaki, X.D. Sun, J. Phys. Chem. C 111 (2007) 4969.
[15] S. Yin, H. Hasegawa, D. Maeda, M. Ishitsuka, T. Sato, J. Photochem. Photobiol. A 163 (2004) 1.
[16] D.V. Goia, J. Mater. Chem. 14 (2004) 451.
[17] M.A. Kipnis, D.A. Agievskii, E.I. Suslova, V.G. Lebedevskaya, F.A. Pogrebnoi, Russ. J. Inorg. Chem. 27 (1982) 1269.
[18] K. Eda, Y. Uno, N. Nagai, N. Sotani, M.S. Whittingham, J. Solid State Chem. 178 (2005) 2791.
[19] Y. Ding, Y. Wan, Y.-L. Min, W. Zhang, S.-H. Yu, Inorg. Chem. 47 (2008) 7813.
[20] F. Izumi, T. Ikeda, Mater. Sci. Forum 321–324 (2000) 198.
[21] R.J.B. Jakeman, M.J. Kwiecien, W.M. Reiff, A.K. Cheetham, C.C. Torardi, Inorg. Chem. 30 (1991) 2806.
[22] U. Kolitsch, K. Schwendtner, Z. Kristallogr. New Cryst. Struct. 219 (2004) 347.
[23] U. Kolitsch, K. Schwendtner, Acta Crystallogr. C 61 (2005) i86–i89.
[24] K. Eda, Y. Uno, N. Nagai, N. Sotani, C. Chen, M.S. Whittingham, J. Solid State Chem. 179 (2006) 1453.
[25] M. Wiesmann, H. Ehrenberg, G. Wltschek, P. Zinn, H. Weitzel, H. Fuss, J. Magn. Magn. Mater. 150 (1995) L1.